

Showcasing research from Prof. Zhongmin Liu's team at Dalian Institute of Chemical Physics, Chinese Academy of Sciences, Dalian, China.

Role of naphthalene during the induction period of methanol conversion on HZSM-5 zeolite

Despite the lower activity of naphthalene compared with that of methylbenzenes, its activity was also proven over an HZSM-5 catalyst. The co-fed naphthalene could act as initial aromatic HCP species and promote the aromatic-based cycle which led to the increase of the C<sub>2</sub>H<sub>4</sub>/C<sub>3</sub>H<sub>6</sub> ratio at low methanol conversion.

As featured in:



See Lei Xu, Zhongmin Liu *et al.*  
*Catal. Sci. Technol.*, 2016, **6**, 3737.



[www.rsc.org/catalysis](http://www.rsc.org/catalysis)

Registered charity number: 207890

CrossMark  
click for updatesCite this: *Catal. Sci. Technol.*, 2016,  
6, 3737

## Role of naphthalene during the induction period of methanol conversion on HZSM-5 zeolite†

Liang Qi,<sup>abc</sup> Jinzhe Li,<sup>ab</sup> Yingxu Wei,<sup>ab</sup> Lei Xu<sup>\*ab</sup> and Zhongmin Liu<sup>\*ab</sup>

The role of methylnaphthalenes in a methanol to hydrocarbons (MTH) reaction on HZSM-5 zeolite was systematically studied on a fixed-bed reaction system. As this is a polycyclic aromatic species, it was interesting to find that co-feeding a small amount of naphthalene could also promote methanol conversion at a low temperature. For the first time, methylnaphthalenes were found to be able to act as initial active HCP species on HZSM-5. The introduced naphthalene could help generate more active methylbenzene HCP species and enhance the aromatic-based cycle during the induction period. As a result, ethene selectivity was promoted due to the co-fed naphthalene. Moreover, despite the large molecular size of naphthalene, it can still function as an active HCP species on the internal acid sites of the HZSM-5 catalyst.

Received 22nd December 2015,  
Accepted 11th March 2016

DOI: 10.1039/c5cy02238j

www.rsc.org/catalysis

### 1. Introduction

As an alternative route for the production of gasoline, light olefins and aromatics from non-oil resources, using methanol to hydrocarbons (MTH) reactions over an acidic zeolite catalyst, including MTG (methanol-to-gasoline), MTO (methanol-to-olefins), MTP (methanol-to-propene) and MTA (methanol-to-aromatics) has received much attention from both academia and industry.<sup>1–12</sup>

Previous studies indicated that the whole MTH reaction is composed of an induction period, a steady-state reaction period and a deactivation period.<sup>1</sup> Up to now, the hydrocarbon pool (HCP) mechanism, an indirect mechanism proposed by Haw and Kolboe, has gained general acceptance based on experimental observations as well as theoretical calculations.<sup>3,13–15</sup> Based on the HCP mechanism, the HCP species has been described as a catalytic scaffold, to which methanol is added and olefins are eliminated in a closed catalytic cycle.<sup>3,14–17</sup> Therefore, the combination of the HCP species and zeolite framework is the actual active catalyst.

Since the proposal of the HCP mechanism, investigation of the intermediates has received great interest.<sup>9,10,18–21</sup> Thus

far, methylbenzenes and the corresponding carbenium ions, typically pentamethylbenzene (pentaMB) and hexamethylbenzene (hexaMB), have been proved to be the main reactive HCP species over SAPO-34 and H-beta catalysts.<sup>17,22–27</sup> While using DNL-6, a SAPO-type molecular sieve with large cavities, a heptamethylbenzenium cation (heptaMB<sup>+</sup>) was directly observed in the methanol conversion.<sup>26</sup> Moreover, heptaMB<sup>+</sup> and a pentamethylcyclopentenyl cation (pentaMCP<sup>+</sup>), were also directly observed in CHA-type catalysts using methanol as the sole reactant.<sup>27</sup> For HZSM-5, in recent years, the higher methylbenzenes (tetramethylbenzenes (tetraMBs) and pentaMB) were shown to be more active than the lower ones (xylene and trimethylbenzene (triMBs)),<sup>28,29</sup> and several dimethylcyclopentenyl carbenium ions (DiMCPs<sup>+</sup>), trimethylcyclopentenyl carbenium ions (triMCPs<sup>+</sup>) and the pentamethylbenzenium ion (pentaMB<sup>+</sup>) were identified as major active intermediates.<sup>29</sup> Besides, Olsbye and co-workers found that other than methylbenzenes, olefins may also act as another kind of active HCP species in zeolites such as the medium-pore HZSM-5 zeolite with 3-D 10-ring channels.<sup>13,30</sup> This leads to the proposal and establishment of the “dual-cycle” mechanism: one cycle in which olefins are repeatedly methylated to form branched species which are susceptible to cracking and another in which aromatics are repeatedly methylated and dealkylated to form light olefins.<sup>13,30–32</sup>

Interestingly, Haw and co-workers found that in addition to PMBs, methylnaphthalenes can also act as active aromatic HCP species in HSAPO-34, thereby exhibiting a high selectivity for ethene. They can play the role of either active olefin-eliminating HCP compounds or as precursors for the deactivating species or coke, *i.e.*, larger aromatic hydrocarbons trapped in the zeolitic pore.<sup>33–36</sup> Recently, it was found that over an HSSZ-13 catalyst, methylated naphthalene

<sup>a</sup> National Engineering Laboratory for Methanol to Olefins, Dalian National Laboratory for Clean Energy, Dalian 116023, People's Republic of China.  
E-mail: liuzm@dicp.ac.cn, leixu@dicp.ac.cn; Fax: +86 411 84379998;  
Tel: +86 411 84379998

<sup>b</sup> iChEM (Collaborative Innovation Center of Chemistry for Energy Materials), Dalian Institute of Chemical Physics, Chinese Academy of Sciences, Dalian 116023, People's Republic of China

<sup>c</sup> University of Chinese Academy of Sciences, Beijing 100049, People's Republic of China

† Electronic supplementary information (ESI) available. See DOI: 10.1039/c5cy02238j

carbocations were active HCP species at high reaction temperatures (623–723 K) while they can also lead to catalyst deactivation at low reaction temperatures (573 and 598 K).<sup>37</sup>

Generally speaking, the possible active aromatic HCP species can be directly investigated by analyzing the “coke” species in the zeolite through a <sup>12</sup>C/<sup>13</sup>C methanol switching experiment. The distribution of retained organics in HSAPO-34 varied from benzene to methylpyrenes, with methylnaphthalenes as the dominating species.<sup>30</sup> Bjorgen *et al.* carefully investigated the coke species formed during the MTH reaction on an HZSM-5 catalyst with different Si/Al ratios (Si/Al = 25, 45, 140) and found that methylbenzenes were the only retained compounds in spite of the varying acid site density. However, a large amount of naphthalene species were directly found in the retained species during the MTH reaction over an HZSM-5 catalyst in our recent work.<sup>38</sup> Moreover, as a medium-pore zeolite, HZSM-5 has been intensively studied as a promising catalyst for the methylation of 2-methylnaphthalene (MN) to selectively synthesize 2,6-dimethylnaphthalene (2,6-DMN), a feedstock of high performance polymeric materials such as polyethylenenaphthalene (PEN).<sup>39,40</sup> This process demonstrates that naphthalene, MN and 2,6-DMN can all diffuse through the ZSM-5 channels successfully in some way.

Despite the abundant existence of methylnaphthalene species retained in the channels of the HZSM-5 catalyst under some conditions, the specific role of them during the MTH reaction is still unclear until now. It's unclear whether the methylnaphthalenes are the active species or deactivating species at low temperature. To clarify this puzzle, in present research, a certain amount of naphthalene was directly introduced in methanol to investigate its effect during the induction period of the MTH reaction over the HZSM-5 catalyst. It was found that the conversion of methanol at low temperature could be evidently promoted through adding a small amount of methylnaphthalene species. Moreover, how and where the polycyclic species function as active HCP species were also investigated in detail. The results help us to understand the HCP mechanism over the HZSM-5 catalyst more comprehensively.

## 2. Experimental section

### 2.1. Preparation of the catalysts

HZSM-5 (Si/Al = 19, 99) (the samples were designated HZ-19 and HZ-99 correspondingly) was obtained from the Catalyst Plant of Nankai University.

The silylated catalyst was prepared as follows: firstly, the HZSM-5 zeolite with a Si/Al ratio of 19 was impregnated with a mixture solution of tetraethoxysilane and ethanol for 12 h at room temperature. Then, the impregnation liquid was removed by filtration. The solid sample was dried at 120 °C for 6 h and then calcined at 550 °C for 4 h in dry air and finally steamed at 650 °C for 4 h to obtain the silylated catalyst.

### 2.2. Characterization of the catalysts

The acid properties were examined by means of the temperature-programmed desorption of ammonia (NH<sub>3</sub>-TPD). The experiment was carried out with Autochem 2920 equipment (Micromeritics). The calcined samples were pretreated at 550 °C for 1 h in He atmosphere and were then saturated with ammonia at 100 °C for 30 min. After the samples were purged with helium, they were heated at 10 °C min<sup>-1</sup> from 100 °C to 700 °C.

*In situ* FTIR spectroscopy experiments of adsorbed pyridine and collidine (2,4,6-trimethylpyridine) were both performed on a TENSOR 27 spectrometer. A self-supporting disk (15–20 mg) of the sample was placed in an IR cell equipped with a vacuum system and pretreated by evacuation (10<sup>-2</sup> Pa) at 450 °C for 1 h. Pyridine was adsorbed on the sample disk at 30 °C for 1 h and then physically desorbed at 200 °C for 1 h. The collidine was adsorbed at 30 °C for 1 h, and the subsequent physical desorption was not needed.

### 2.3. Catalytic studies

The HZ-19 and HZ-99 samples were pressed into tablets, crushed and sieved into a fraction of 40–60 mesh. Methanol (>99.9%), naphthalene (AR), MN (>96%) and 2,6-DMN (>98%) were all purchased from commercial sources and were of the highest purity available. The reactions were performed in a fixed-bed stainless steel tubular reactor (9 mm i.d.) at atmospheric pressure. In all experiments, a catalyst sample of 1.0 g was loaded into the reactor. Then quartz sand was added to the upper and lower part of reactor to get a plug flow of the mixed feed. Prior to the introduction of the reactants, the catalyst was activated *in situ* at 550 °C under a flow of 20 ml min<sup>-1</sup> helium for 1 h before cooling to reaction temperatures. The reactant was pumped into the reactor at a certain and steady velocity (0.085 ml min<sup>-1</sup>). The effluent was analyzed by an on-line gas chromatograph (Agilent GC7890A) equipped with a FID detector and a PorAPLOT Q-HT capillary column.

The conversion in this context refers to the percentage of methanol converted into hydrocarbons, and dimethylether is also considered as a reactant.

### 2.4. Extraction and GC-MS analysis of the confined organics

Organic compounds trapped in the catalyst were obtained by first dissolving the catalyst (50 mg) in 1.0 mL of 15% HF in a screw-cap Teflon. The organic phase was extracted by dichloromethane (CH<sub>2</sub>Cl<sub>2</sub>), and then analyzed using an Agilent 7890 A/5975C GC/MSD.

### 2.5. <sup>12</sup>C/<sup>13</sup>C-methanol switch experiment

In the <sup>12</sup>C/<sup>13</sup>C-methanol switch experiments, after co-feeding <sup>12</sup>C-methanol with 1 wt% naphthalene at 250 °C for 40 min, the feeding of <sup>12</sup>C-methanol was stopped and was switched to <sup>13</sup>C-methanol for a further 2 min. The isotopic distribution

of the materials confined in the catalyst were determined by GC-MS (Agilent 7890/5975C).

### 3. Results and discussion

#### 3.1. Effects of co-feeding naphthalene on the methanol conversion during the MTH induction period

For the methanol conversion reaction over the HZ-19 catalyst at 250 °C, a long induction period is clearly shown in Fig. 1(a). Almost no apparent methanol conversion could be observed before 200 min, indicating that the generation of HCP species was quite difficult at a low reaction temperature.<sup>41</sup> The methanol conversion increased slowly to about 5% after 400 min.

Naphthalene was then co-fed with methanol in a mass ratio of 1% (wt%) to investigate its effect on the MTH reaction over HZSM-5. It should be pointed out that a low concentration of naphthalene was co-fed in this study to avoid the methylation of aromatics rather than the methanol conversion becoming the main catalytic reaction. It's clearly shown that the methanol conversion reaction was promoted by co-feeding the small amount of naphthalene (Fig. 1(a)). The conversion of methanol increased quickly from 1.2% to 10% in 60 min suggesting an obvious promoting effect of naphthalene on the MTH reaction. Thus it can be speculated that naphthalene can act as an active HCP species on its own or it can promote the formation of other active HCP species during the MTH reaction.

To further consolidate our proposal, a similar experiment was performed on the HZ-99 catalyst at 290 °C (Fig. 1(b)). Due to its low acid site density (Fig. S1†), the HZ-99 catalyst showed relatively low catalytic activity even at a higher temperature (290 °C)—almost no apparent methanol conversion (<1%) was observed during the whole reaction process. However, after the addition of naphthalene, the methanol conversion increased quickly from 7% to 22% in 60 min, presenting a similar promoting effect of naphthalene on methanol conversion to that on the HZ-19 catalyst.

The influence of the concentration of naphthalene on the MTH induction period was also investigated on the HZ-19 catalyst. The naphthalene co-feeding concentration was var-

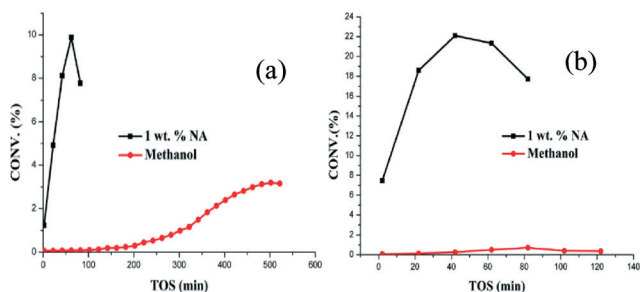


Fig. 1 Methanol conversion profiles as a function of time on stream (TOS) with the pure methanol feed and methanol co-fed with 1% (wt%) naphthalene at 250 °C on the HZ-19 catalyst (a), and at 290 °C on the HZ-99 catalyst (b).

ied from 0.1 to 1 wt%. As shown in Fig. 2, the initial methanol conversion was elevated from 0 to 1.2% and the methanol conversion reaction was accelerated continuously with the increase of naphthalene concentration. However, it was also found that the methanol conversion started to decrease much earlier with the increase of the naphthalene co-feeding concentration, indicating an easier deactivation of the catalyst. Based on the above results, it is suggested that naphthalene can play a role of either an active HCP compound or a precursor for the deactivating species or coke, *i.e.*, larger aromatic hydrocarbons trapped in the HZSM-5 zeolite.<sup>33–36</sup>

#### 3.2. Effects of co-feeding naphthalene on the product distribution and the C<sub>2</sub>H<sub>4</sub>/C<sub>3</sub>H<sub>6</sub> ratio during the MTH induction period

The effect of co-feeding naphthalene on the product distribution in the MTH reaction was also investigated. The product distribution as a function of TOS at 250 °C is shown in Fig. 3. Under pure methanol feeding conditions (Fig. 3(a)), methane and ethene were the only initially detectable products and C<sub>3</sub>H<sub>6</sub>, C<sub>4</sub>, C<sub>5</sub> and C<sub>6</sub><sup>+</sup> species also appeared in the following time. The selectivity of all the products would reach equilibrium later in the autocatalysis reaction stage. The results are in accordance with our recently published work.<sup>41</sup>

For the naphthalene co-feeding experiments, C<sub>3</sub>H<sub>6</sub>, C<sub>4</sub>, C<sub>5</sub> and C<sub>6</sub><sup>+</sup> species appeared much earlier in the co-feeding process, which demonstrated the promoting effect of naphthalene on the methanol conversion reaction (Fig. 3(b)–(d)). However, no obvious change can be observed in the selectivity of all the products during the autocatalysis reaction stage except with the different feeding conditions.

According to a recent report, the selectivity to methane, ethene and aromatics could be elevated at the expense of the selectivity to propene and C<sub>4</sub><sup>+</sup> higher olefins in the MTH reaction process when co-feeding low methylbenzenes (benzene, toluene and xylenes) with methanol.<sup>18,42</sup> It has been demonstrated that co-feeding low methylbenzenes propagates

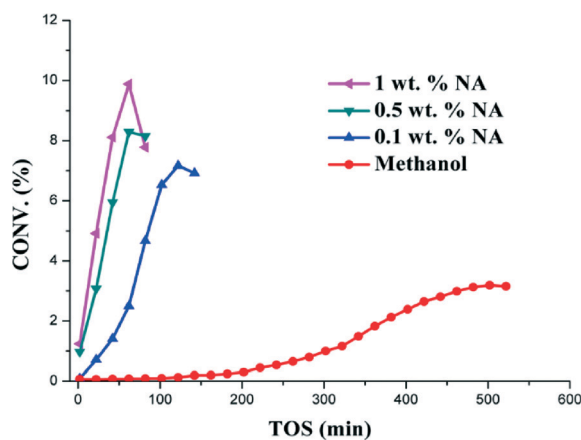


Fig. 2 Methanol conversion profiles as a function of TOS for methanol co-feeding with different profiles amounts of naphthalene at 250 °C on the HZ-19 catalyst.

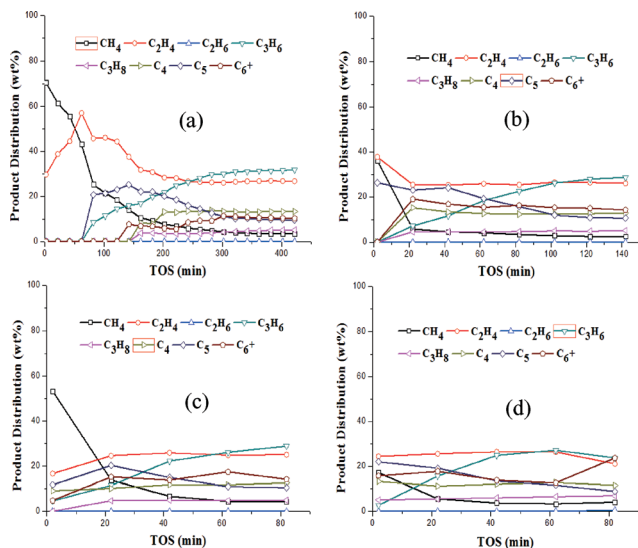


Fig. 3 Product distribution versus TOS for the reactions of methanol alone (a) and methanol co-feeding with different amounts of naphthalene: 0.1 wt% (b), 0.5 wt% (c), 1 wt% (d) at 250 °C.

the aromatic-based cycle *via* aromatic methylation and elimination of light olefins while suppressing the olefin-based cycle.<sup>18,42</sup> Haw and co-workers proved that methylnaphthalenes can act as active HCP species and exhibit a high selectivity for ethene in HSAPO-34.<sup>33,34</sup> In this work, the selectivity to ethene and propene is almost unchanged during the autocatalysis reaction stage under different feeding conditions. However, if we focus on the influence of the co-fed naphthalene on the C<sub>2</sub>H<sub>4</sub>/C<sub>3</sub>H<sub>6</sub> ratio during the initial stage of the methanol conversion reaction (methanol conv. = 1%) at 250 °C, it could be found that the C<sub>2</sub>H<sub>4</sub>/C<sub>3</sub>H<sub>6</sub> ratio increased from 1 to 9 as the naphthalene co-feeding concentration increased from 0 to 1 wt% (Fig. 4).

As reported, propene is much more easily methylated to form long-chain olefins compared to ethene.<sup>43</sup> Moreover, long-chain olefins will further undergo cyclization and aromatization reactions to form methylbenzene which can act as

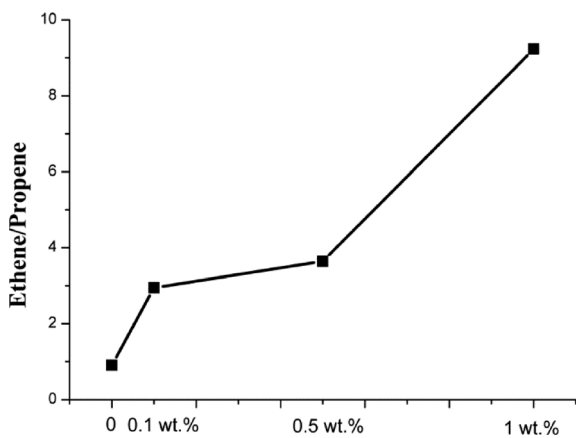


Fig. 4 Ethene/propene ratios at different feeding conditions when methanol conv. = 1% at 250 °C for the HZ-19 catalyst.

an aromatic HCP species. During the induction period, a sufficient amount of aromatic HCP species should accumulate to initiate the MTH reaction.<sup>41</sup> So, the aromatic-based cycle should be more dominant during this stage and as a result, the C<sub>2</sub>H<sub>4</sub>/C<sub>3</sub>H<sub>6</sub> ratio was always greater than one during the induction period. Taking the “dual-cycle” MTH mechanism on the HZSM-5 catalyst into consideration, the addition of naphthalene may help generate more aromatic HCP species and make the aromatic-based cycle proceed relatively easily in the initial stage. The formed methylbenzene is more inclined to promote the formation of ethene than propene and thus leads to the increase of the C<sub>2</sub>H<sub>4</sub>/C<sub>3</sub>H<sub>6</sub> ratio with the increasing concentration of the co-fed naphthalene.

### 3.3. Effects of co-feeding naphthalene on the formation of coke species during the MTH induction period

In order to further clarify how the co-fed naphthalene participates in the MTH reaction and promotes the aromatic-based cycle, the coke species generated during the MTH reaction process were investigated in detail. For the pure methanol conversion at 250 °C for 60 min (Fig. 5(a)), the concentration of retained organics was very low and pentaMB was the most abundant, followed by hexaMB. Hydrocarbons with greater molecular mass than hexaMB were not detected. Similar results have been shown but with hexaMB as the dominating species.<sup>30</sup>

The GC-MS results of co-processing methanol with naphthalene (0.5 and 1 wt%) for a reaction time of 60 min at 250 °C were also investigated (Fig. 5(d) and (e)). It is clearly shown that pentaMB and hexaMB were still the dominant species. The concentration of retained organics increased obviously with the increase of naphthalene concentration, indicating that the co-fed naphthalene promoted the generation of HCP species during the MTH reaction process on the HZSM-5 catalyst. This also corresponds well with the change

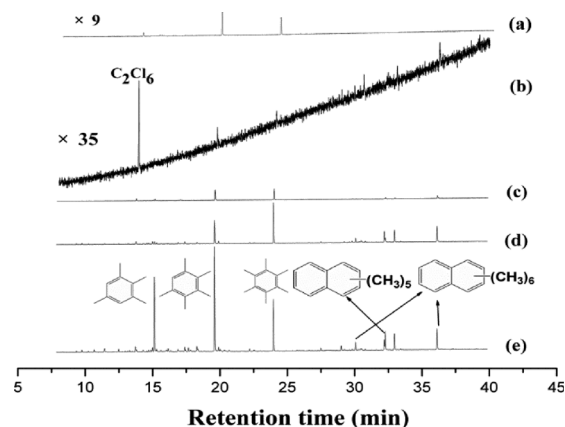


Fig. 5 GC-MS analysis of the retained material in the catalyst at 250 °C for different feeding conditions and reaction time: (a) pure methanol, 60 min; (b) 0.5 wt% naphthalene, 5 min; (c) 0.5 wt% naphthalene, 40 min; (d) 0.5 wt% naphthalene, 60 min; (e) 1 wt% naphthalene, 60 min ((a) and (b) are shown at higher sensitivities; 9× and 35×).

of methanol conversion shown in Fig. 2. Moreover, tetramethylbenzenes (tetraMBs) and a small amount of trimethylbenzenes (triMBs) were also detected. It is worth noting that besides polymethylbenzenes (polyMBs), a certain amount of methylnaphthalenes emerged which were not detected under conditions without co-feeding with naphthalene (Fig. 5(a)).

To further clarify the effect of naphthalene on the formation of coke species in the MTH reaction, a series of experiments with an extended reaction time (5 min, 40 min and 60 min) were performed by co-feeding methanol with naphthalene (0.5 wt%). The results are also shown in Fig. 5. The concentration of all aromatics increased consistently up to 60 min. At 5 min, the retained coke species were mainly methylnaphthalenes (>50%) and the concentration of polyMBs was relatively low (Fig. 5(b)). When the reaction time was prolonged to 40 min, the concentration of both polyMBs and methylnaphthalenes increased and the amount of polyMBs began to dominate. When the reaction time was further prolonged to 60 min, the total amount of aromatics continued increasing and polyMBs became the dominating coke species, especially pentaMB.

Taking all the results of the coke analysis into consideration, it can be found that the methylnaphthalene species cannot be formed at low temperature (250 °C) under the pure methanol feeding condition (Fig. 5(a)). So, the appearance of methylnaphthalene species in the naphthalene co-feeding experiments (Fig. 5(b)–(e)) indicated that the naphthalene was involved in the methanol conversion reaction. Moreover, the higher concentration of the coke species for the co-feeding experiments helped to prove that the co-fed naphthalene could promote the generation of aromatic HCP species, especially higher methylbenzene products. According to recent research, higher methylbenzenes (tetraMB and pentaMB) were identified as the major active HCP species over the HZSM-5 catalyst.<sup>28,29</sup> As a result, for the naphthalene co-feeding MTH reaction over the HZSM-5 catalyst, the introduced naphthalene mainly acts as the initial active HCP species, and the main active HCP species should be the later formed higher methylbenzenes.

To further prove this proposal, a <sup>13</sup>C methanol and <sup>12</sup>C naphthalene co-feeding experiment was performed to investigate the relation between the initially introduced naphthalene and the later formed methylbenzenes. After converting a mixture of <sup>13</sup>C methanol and natural abundance naphthalene at 250 °C for 20 min, the isotopic distributions of the main retained species were carefully analyzed (Fig. 6). It can be seen clearly that almost all the methyl groups of the pentamethylnaphthalenes (pentaNAs) and hexamethylnaphthalenes (hexaNAs) were labelled with <sup>13</sup>C atoms, indicating their active participation in the methanol conversion reaction. Moreover, despite the fact that most of the <sup>13</sup>C atoms incorporated into the methylnaphthalenes were located in the methyl group, there was a small amount of <sup>13</sup>C atoms incorporated into the benzene ring. It's worth noting that a certain amount of <sup>12</sup>C atoms in pentaMB and hexaMB also existed, which undoubtedly came from the introduced

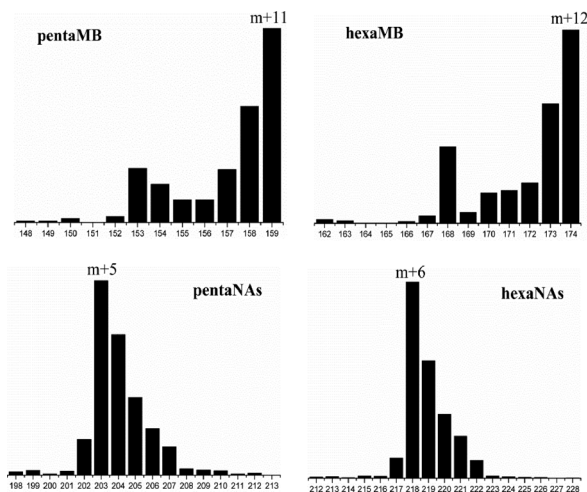


Fig. 6 Isotopic distributions of the retained organic material after co-feeding <sup>13</sup>C methanol and 1 wt% <sup>12</sup>C naphthalene at 250 °C for 20 min.

naphthalene. The results imply that naphthalene can act as an aromatic HCP species. Compared with the pure methanol conversion reaction, the introduced naphthalene may firstly promote the generation of olefins, and the olefin products can then be converted to the methylbenzene HCP species. As a result, the introduced naphthalene can promote the formation of methylbenzenes and accelerate the methanol conversion reaction apparently.

#### 3.4. Effect of co-feeding different aromatic compounds on the methanol conversion during the MTH induction period

The reactivity of methylbenzenes and naphthalene was directly compared under the same reaction conditions using benzene and naphthalene as the co-feeding aromatic species respectively (Fig. 7). It is clearly seen that the methanol conversion increased more quickly and the maximum methanol conversion was much higher under the benzene co-feeding conditions, presenting a more effective autocatalytic activity than that of naphthalene. Moreover, it has been proven that

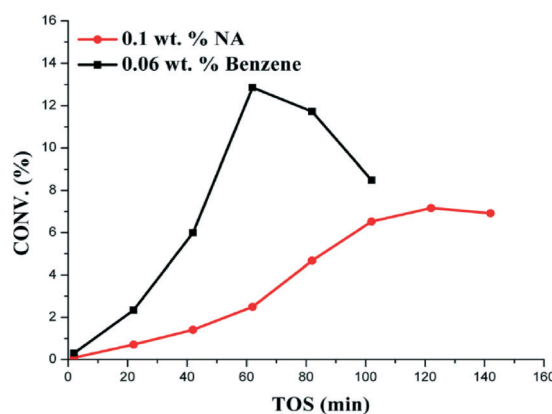


Fig. 7 Methanol conversion profiles as a function of TOS for co-feeding naphthalene and benzene at 250 °C on the HZ-19 catalyst.

the reactivity of higher methylbenzenes is much higher than their lower counterparts.<sup>28,29</sup> So, the reactivity of the retained coke species over the HZSM-5 catalyst may be: higher methylbenzenes > lower methylbenzenes > methylnaphthalenes.

<sup>12</sup>C/<sup>13</sup>C-methanol switch experiments were also conducted to investigate the reactivity of methylbenzenes and methylnaphthalenes in the catalyst during methanol conversion. The major retained species after co-feeding methanol with 1 wt% naphthalene for 40 min is presented in Fig. S2.† The isotopic distribution as well as the total <sup>13</sup>C content of the retained organic materials on the catalyst after the switch experiments is shown in Fig. 8. Among the retained organics, it can be obviously seen that methylbenzenes exhibited a much higher <sup>13</sup>C content than that of methylnaphthalenes, implying their higher reactivity as important intermediates during the MTH reaction. Moreover, it can be seen that the reactivity of methylnaphthalenes was in the order of pentaNAs > hexaNAs > heptaNAs. It can be finally concluded that for the naphthalene co-feeding system over the HZSM-5 catalyst, on one hand, naphthalene could act as an initial HCP species and promote the generation of higher methylbenzenes which would act as more reactive reaction centers in the following MTH process, and on the other hand, a certain amount of accumulated methylnaphthalene species in the zeolite could also act as deactivating species at low temperature due to their large molecular size.

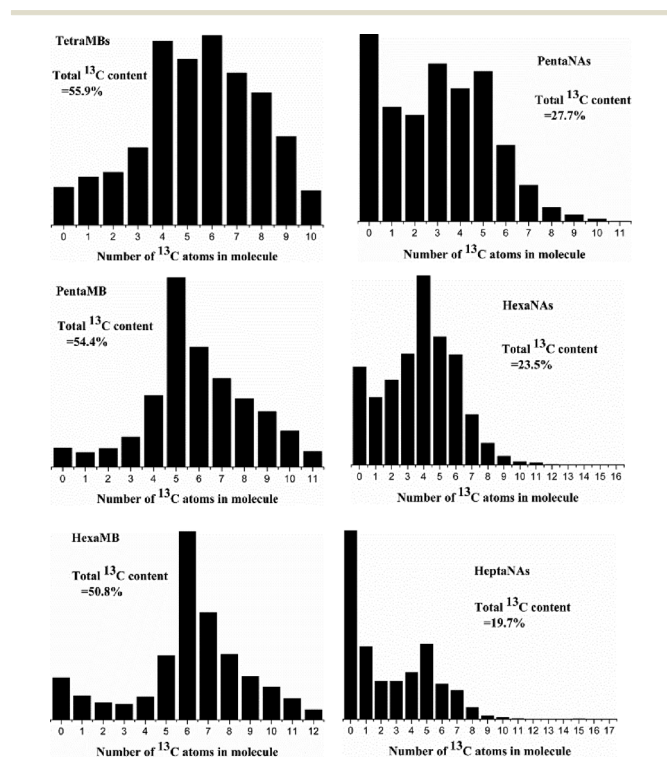


Fig. 8 Isotopic distributions of the retained organic materials after the <sup>12</sup>C/<sup>13</sup>C switch experiment at 250 °C: co-feeding <sup>12</sup>C-methanol and 1 wt% naphthalene for 40 min during the MTH reaction, followed by 2 min of <sup>13</sup>C-methanol feeding. The total <sup>13</sup>C content of each molecule was marked in each picture.

Considering that 2-methylnaphthalene (MN) and 2,6-dimethylnaphthalene (2,6-DMN) can also diffuse in the channels of the HZSM-5 zeolite, the same molar concentrations (0.4 mol%) of naphthalene, MN and 2,6-DMN were each introduced to methanol to compare their promoting effect on the methanol conversion reaction. It can be seen from Fig. 9 that MN showed the best promoting effect followed by naphthalene and 2,6-DMN. The possible reasons were that fewer methylation steps were needed to complete the catalytic cycle for MN and there was a larger diffusivity hindrance for 2,6-DMN.

### 3.5. Effect of naphthalene on the internal acid sites

Song *et al.* found that it was the external acid sites and pore mouth catalysis that played a key role in the production of the initial olefins on the HZSM-22 catalyst.<sup>44</sup> Moreover, for HZSM-5, the aromatic HCP species are considered to function at the intersections of the catalyst. Considering the confined space of the intersection of HZSM-5 for naphthalene, it is also necessary to clarify whether the naphthalene can work at the internal acid sites. To carry out this investigation, the acid sites on the external surface should be removed.

The acid sites of the external surface of HZSM-5 could be removed selectively through surface silylation as reported in our former work.<sup>38</sup> After silylation, the acid properties of the common HZSM-5 and the silylated one were directly investigated through FT-IR with different adsorbed probe molecules. As is shown in Fig. 10(a), three pyridine adsorption peaks at 1545, 1489 and 1454 cm<sup>-1</sup> are observed for both the common HZ-19 and silylated HZ-19 which are assigned to the Brønsted acid sites, the Lewis combined with Brønsted acid sites and the Lewis acid sites respectively.<sup>45</sup> It is worth noting that the intensity of the peaks at 1545 cm<sup>-1</sup> and 1454 cm<sup>-1</sup> for the silylated HZ-19 decreased apparently, while the intensity of the peak at 1489 cm<sup>-1</sup> remained almost the same. Therefore, it can be concluded that the silylation treatment is able to etch most of the Lewis and Brønsted acid sites on or near the external surface. In order to further investigate the

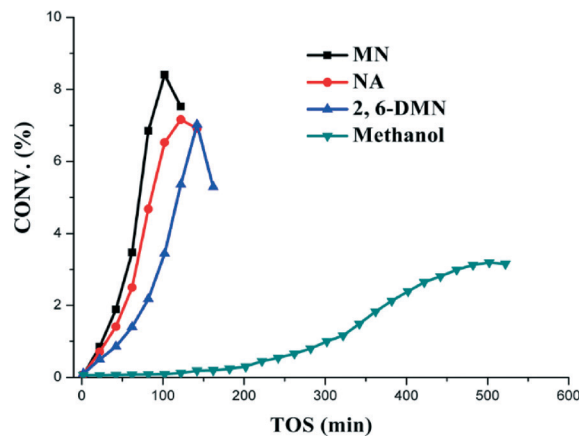


Fig. 9 Methanol conversion profiles as a function of TOS for different co-feeding conditions at 250 °C on the HZ-19 catalyst.

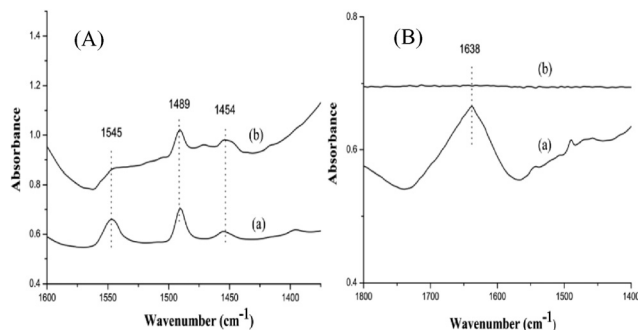


Fig. 10 FT-IR spectra of (A) pyridine-adsorbed and (B) collidine-adsorbed (a) common HZ-19 and (b) silylated HZ-19. Spectra in panels A and B were obtained by the subtraction of background spectra from those measured after adsorption and physical desorption procedures.

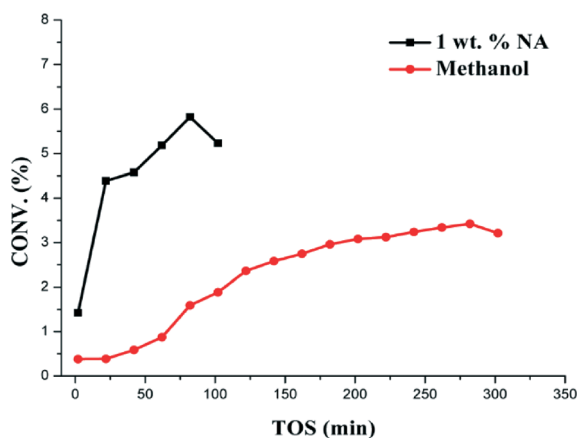


Fig. 11 Methanol conversion profiles as a function of TOS for pure methanol feed and methanol co-fed with 1% naphthalene at 320 °C on silylated HZ-19.

acid sites of the internal and external surfaces, collidine was chosen as the probe molecule. Because of the larger molecular size of collidine than the pore size of ZSM-5, it should be adsorbed only at the acid sites on the external surface.<sup>46–48</sup> As is shown in Fig. 10(b), the peak at 1638  $\text{cm}^{-1}$  associated with collidine adsorbed on the Lewis acid sites for the silylated HZ-19 disappeared completely, suggesting that the acid sites on the external surface were removed after silanization. These results indicated that the silanization method in the present study is an effective method to eliminate acid sites on the external surface.

The activity of the silylated HZ-19 was investigated and the results are shown in Fig. 11. The catalyst activity was found to decrease after silanization and the maximum methanol conversion was less than 4% even at a higher temperature (320 °C) (Fig. 11). This demonstrated that the silanization treatment may also etch some of the internal acid sites near the pore mouth. However, the promoting effect of naphthalene on the methanol conversion reaction was still obvious when co-feeding 1% naphthalene with methanol. Combining the above results it can be concluded that naphthalene can act as an active HCP species on the internal acid sites. The naphthalene may function as an active auto-

catalytic species at the pore mouth or the intersection acid sites of the zeolite through the HCP mechanism. However, whether the naphthalene can function at the external surface acid sites is still unclear and needs further research in a following study.

## 4. Conclusions

An HZSM-5 catalyst containing an initial polycyclic aromatic reaction center during a MTH reaction was investigated. Co-feeding naphthalene was found to accelerate the formation of methylbenzene HCP species and thus shorten the MTH induction period. Although the activity of the introduced naphthalene was proved to be much lower than that of the methylbenzenes, its activity at a low reaction temperature was found for the first time over a HZSM-5 catalyst. The co-fed naphthalene could act as an initial aromatic HCP species and promote the aromatic-based cycle which lead to the increase of the  $\text{C}_2\text{H}_4/\text{C}_3\text{H}_6$  ratio at a low methanol conversion. A certain amount of methylnaphthalene species will also lead to the catalyst deactivation at a low reaction temperature. More interestingly, despite the large molecular size of naphthalene, it can function as a HCP species on the internal acid sites of the HZSM-5 catalyst. These findings help us understand the role of aromatics in the HCP mechanism more comprehensively.

## Acknowledgements

The authors thank the financial support from the National Natural Science Foundation of China (No. 21576256 and No. 21273005).

## Notes and references

- P. Tian, Y. Wei, M. Ye and Z. Liu, *ACS Catal.*, 2015, 5, 1922–1938.
- M. Stocker, *Microporous Mesoporous Mater.*, 1999, 29, 3–48.
- J. F. Haw, W. G. Song, D. M. Marcus and J. B. Nicholas, *Acc. Chem. Res.*, 2003, 36, 317–326.
- K. Y. Lee, H. K. Lee and S. K. Ihm, *Top. Catal.*, 2010, 53, 247–253.
- U. Olsbye, M. Bjorgen, S. Svelle, K. P. Lillerud and S. Kolboe, *Catal. Today*, 2005, 106, 108–111.
- W. Wang, Y. J. Jiang and M. Hunger, *Catal. Today*, 2006, 113, 102–114.
- J. L. White, *Catal. Sci. Technol.*, 2011, 1, 1630–1635.
- D. Chen, K. Moljord and A. Holmen, *Microporous Mesoporous Mater.*, 2012, 164, 239–250.
- U. Olsbye, S. Svelle, M. Bjorgen, P. Beato, T. V. W. Janssens, F. Joensen, S. Bordiga and K. P. Lillerud, *Angew. Chem., Int. Ed.*, 2012, 51, 5810–5831.
- K. Hemelsoet, J. Van der Mynsbrugge, K. De Wispelaere, M. Waroquier and V. Van Speybroeck, *ChemPhysChem*, 2013, 14, 1526–1545.
- S. Ilias and A. Bhan, *ACS Catal.*, 2013, 3, 18–31.
- J. R. Chen, J. Z. Li, C. Y. Yuan, S. T. Xu, Y. X. Wei, Q. Y. Wang, Y. Zhou, J. B. Wang, M. Z. Zhang, Y. L. He, S. L. Xu and Z. M. Liu, *Catal. Sci. Technol.*, 2014, 4, 3268–3277.



- 13 S. Svelle, F. Joensen, J. Nerlov, U. Olsbye, K. P. Lillerud, S. Kolboe and M. Bjorgen, *J. Am. Chem. Soc.*, 2006, **128**, 14770–14771.
- 14 I. M. Dahl and S. Kolboe, *J. Catal.*, 1996, **161**, 304–309.
- 15 I. M. Dahl and S. Kolboe, *J. Catal.*, 1994, **149**, 458–464.
- 16 I. M. Dahl and S. Kolboe, *Catal. Lett.*, 1993, **20**, 329–336.
- 17 W. G. Song, J. F. Haw, J. B. Nicholas and C. S. Heneghan, *J. Am. Chem. Soc.*, 2000, **122**, 10726–10727.
- 18 S. Ilias and A. Bhan, *J. Catal.*, 2012, **290**, 186–192.
- 19 M. Westgard Erichsen, S. Svelle and U. Olsbye, *J. Catal.*, 2013, **298**, 94–101.
- 20 S. Ilias and A. Bhan, *J. Catal.*, 2014, **311**, 6–16.
- 21 K. De Wispelaere, K. Hemelsoet, M. Waroquier and V. Van Speybroeck, *J. Catal.*, 2013, **305**, 76–80.
- 22 B. Arstad and S. Kolboe, *J. Am. Chem. Soc.*, 2001, **123**, 8137–8138.
- 23 B. Arstad and S. Kolboe, *Catal. Lett.*, 2001, **71**, 209–212.
- 24 M. Bjorgen, F. Bonino, S. Kolboe, K. P. Lillerud, A. Zecchina and S. Bordiga, *J. Am. Chem. Soc.*, 2003, **125**, 15863–15868.
- 25 J. B. Nicholas, A. A. Kheir, T. Xu, T. R. Krawietz and J. F. Haw, *J. Am. Chem. Soc.*, 1998, **120**, 10471–10481.
- 26 J. Z. Li, Y. X. Wei, J. R. Chen, P. Tian, X. Su, S. T. Xu, Y. Qi, Q. Y. Wang, Y. Zhou, Y. L. He and Z. M. Liu, *J. Am. Chem. Soc.*, 2012, **134**, 836–839.
- 27 S. T. Xu, A. M. Zheng, Y. X. Wei, J. R. Chen, J. Z. Li, Y. Y. Chu, M. Z. Zhang, Q. Y. Wang, Y. Zhou, J. B. Wang, F. Deng and Z. M. Liu, *Angew. Chem., Int. Ed.*, 2013, **52**, 11564–11568.
- 28 H. G. Jang, H. K. Min, S. B. Hong and G. Seo, *J. Catal.*, 2013, **299**, 240–248.
- 29 C. Wang, Y. Y. Chu, A. M. Zheng, J. Xu, Q. Wang, P. Gao, G. D. Qi, Y. J. Gong and F. Deng, *Chem – Eur J.*, 2014, **20**, 12432–12443.
- 30 M. Bjorgen, S. Svelle, F. Joensen, J. Nerlov, S. Kolboe, F. Bonino, L. Palumbo, S. Bordiga and U. Olsbye, *J. Catal.*, 2007, **249**, 195–207.
- 31 S. Svelle, U. Olsbye, F. Joensen and M. Bjorgen, *J. Phys. Chem. C*, 2007, **111**, 17981–17984.
- 32 M. Bjørgen, F. Joensen, K.-P. Lillerud, U. Olsbye and S. Svelle, *Catal. Today*, 2009, **142**, 90–97.
- 33 H. Fu, W. G. Song and J. F. Haw, *Catal. Lett.*, 2001, **76**, 89–94.
- 34 W. G. Song, H. Fu and J. F. Haw, *J. Phys. Chem. B*, 2001, **105**, 12839–12843.
- 35 K. Hemelsoet, A. Nollet, M. Vandichel, D. Lesthaeghe, V. Van Speybroeck and M. Waroquier, *ChemCatChem*, 2009, **1**, 373–378.
- 36 K. Hemelsoet, A. Nollet, V. Van Speybroeck and M. Waroquier, *Chem – Eur J.*, 2011, **17**, 9083–9093.
- 37 E. Borodina, F. Meirer, I. Lezcano-Gonzalez, M. Mokhtar, A. M. Asiri, S. A. Al-Thabaiti, S. N. Basahel, J. Ruiz-Martinez and B. M. Weckhuysen, *ACS Catal.*, 2015, **5**, 992–1003.
- 38 Y. Bi, Y. L. Wang, Y. X. Wei, Y. L. He, Z. X. Yu, Z. M. Liu and L. Xu, *ChemCatChem*, 2014, **6**, 713–718.
- 39 L. J. Jin, Y. M. Fang and H. Q. Hu, *Catal. Commun.*, 2006, **7**, 255–259.
- 40 L. J. Jin, X. J. Zhou, H. Q. Hu and B. Ma, *Catal. Commun.*, 2008, **10**, 336–340.
- 41 L. Qi, Y. X. Wei, L. Xu and Z. M. Liu, *ACS Catal.*, 2015, **5**, 3973–3982.
- 42 X. Y. Sun, S. Mueller, H. Shi, G. L. Haller, M. Sanchez-Sanchez, A. C. van Veen and J. A. Lercher, *J. Catal.*, 2014, **314**, 21–31.
- 43 V. Van Speybroeck, J. Van der Mynsbrugge, M. Vandichel, K. Hemelsoet, D. Lesthaeghe, A. Ghysels, G. B. Marin and M. Waroquier, *J. Am. Chem. Soc.*, 2011, **133**, 888–899.
- 44 F. F. Wei, Z. M. Cui, X. J. Meng, C. Y. Cao, F. S. Xiao and W. G. Song, *ACS Catal.*, 2014, **4**, 529–534.
- 45 R. Byggningsbacka, L. E. Lindfors and N. Kumar, *Ind. Eng. Chem. Res.*, 1997, **36**, 2990–2995.
- 46 S. Inagaki, S. Shinoda, Y. Kaneko, K. Takechi, R. Komatsu, Y. Tsuboi, H. Yamazaki, J. N. Kondo and Y. Kubota, *ACS Catal.*, 2013, **3**, 74–78.
- 47 M. S. Holm, S. Svelle, F. Joensen, P. Beato, C. H. Christensen, S. Bordiga and M. Bjorgen, *Appl. Catal., A*, 2009, **356**, 23–30.
- 48 F. Thibault-Starzyk, A. Vimont and J. P. Gilson, *Catal. Today*, 2001, **70**, 227–241.